Electronic Supplementary Material (ESI) for RSC Advances.
This journal is © The Royal Society of Chemistry 2016

Supplementary Information

Controlling the Excitation of Radially Polarized Conical Plasmons in Plasmonic Tips in Liquids

Bayarjargal N. Tugchin, Norik Janunts, Michael Steinert, Kay Dietrich, Dmitry Sivun, Siddharth Ramachandran, Khachatur V. Nerkararyan, Andreas Tünnermann, and Thomas Pertsch

S1. DISPERSION RELATION EQUATIONS

First, we look at the plasmonic tip that can be seen as a Kretschmann configuration in conical geometry. Figure S1a illustrates the plasmonic tip and the excitation process of the conical surface plasmon (Co-SP) mode. As shown in the figure, the plasmonic tip[1] is a tapered and fully metal-coated vortex fiber. The radially polarized waveguide (WG) mode within the tapered fiber resonantly excites the radially polarized fundamental Co-SP mode on the gold surface. Then, the plasmonic mode propagates to the apex and creates hot-spot. We are particularly interested in the radially polarized modes because the fundamental Co-SP or the superfocusing mode is radially polarized and has no cutoff.[2]

The coupling between the WG and Co-SP modes is achieved by fulfilling the nonorthogonality relation and phase matching condition. To excite the radially polarized Co-SP mode (TM_0), we choose the radially polarized WG mode of the fiber (TM_{01}) that is nonorthogonal to the Co-SP mode. Figure S1b presents the evolution of effective indices (dashed lines) and amplitudes (solid lines) of the waveguide (red) and Co-SP (blue) modes during propagation toward the tip apex. Parameters used in calculation are a gold coating of 100 nm, a surrounding media refractive index (n_{surr}) of 1, a prism and WG refractive index (n_{prism} and n_{wg}) of 1.4474, a laser wavelength (λ_0) of 784 nm, and a gold refractive index of $n_{gold}^2 = -20.95+1.68i$.[3].

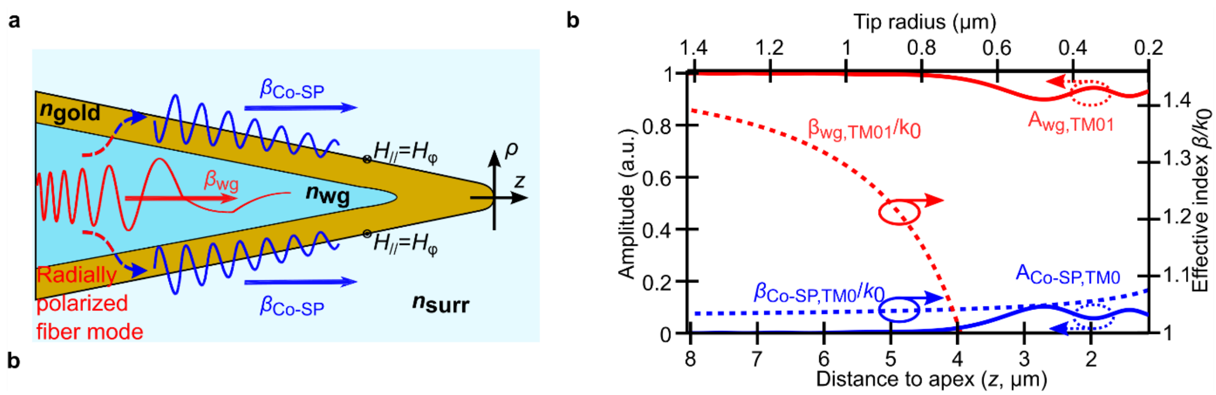

Figure S1. (a) Plasmonic tip illustration. (b) Amplitudes (solid) and effective indices (real part, dashed) of the waveguide (WG, red) and Co-SP (blue) modes versus distance to apex. Amplitudes of WG ($A_{wg,TM01}$) and Co-SP modes ($A_{Co\text{-}SP,TM0}$) are in red and blue solid lines, respectively. Real parts of the effective indices are in red and blue dashed lines for WG ($\beta'_{wg,TM01}/k_0$) and Co-SP modes ($\beta'_{Co\text{-}SP,TM0}/k_0$), respectively. TM_{01} and TM_0 denote the radially polarized waveguide and Co-SP modes. Parameters used for calculation are: the free space wavelength of $\lambda_0 = 784$ nm; the gold coating thickness of 100 nm; the full cone angle of 20°; and structure refractive indices are $n_{prism,wg} = 1.4474$, $n_{gold}^2 = -20.95+1.68i$,[3] and $n_{surr} = 1$.

The effective indices are found from the dispersion relation equations for the radially polarized WG and Co-SP modes. For a gold thickness of 100 nm, we consider the WG and Co-SP modes are weakly coupled; thus, the modes are considered separately. The Co-SP mode is guided in a waveguide with a metal core and a dielectric (surrounding medium) cladding. Meanwhile, the WG mode is in a waveguide with a dielectric (at the tip end, it is mostly vortex fiber cladding) core and a metal cladding. For adiabatic propagation, the conical structure can be considered as consequent cylinders with decreasing radius and infinitesimal height. Essentially, the local cylindrical modes compose the conical modes. At given tip radius, the dispersion relation for the radially polarized WG modes TM_{0p} (where 0 is the azimuthal and p is the radial mode order) is given as[4]

$$\frac{q}{n_{\mathrm{wg}}^2}\frac{J_0(q(b-\Delta))}{J_1(q(b-\Delta))} = i\frac{\chi_2}{n_{\mathrm{gold}}^2}\frac{H_0^{(1)}(i\chi_2(b-\Delta))}{H_1^{(1)}(i\chi_2(b-\Delta))}. \qquad \text{[S1]}$$

Here, the transversal wavevectors are $q^2 = n_{\mathrm{wg}}^2 k_0^2 - \beta_{\mathrm{wg}}^2$ and $\chi_2^2 = \beta_{\mathrm{wg}}^2 - n_{\mathrm{gold}}^2 k_0^2$, $k_0 = 2\pi/\lambda_0$ is the vacuum wavevector with a free space wavelength of λ_0, and β_{wg} is the propagation constant of the waveguide mode. Moreover, b is the tip radius that includes the gold coating thickness of Δ. Meanwhile, $J_m(x)$ is the m^{th} order Bessel function of the 1st kind, and $H_m^{(1)}(x)$ is the m^{th} order Hankel function of the 1nd kind. Among TM_{0p} modes, the cutoff radius (about 708 nm) is the smallest for TM_{01} thus nearest to the tip apex. Therefore, without loss of generality, we assume that the 1st azimuthal order radially polarized waveguide mode (TM_{01}) excites the fundamental radially polarized plasmon mode (TM_0). The dispersion relation for the radially polarized Co-SP mode (TM_0) is given as[5]

$$\frac{\chi_2'}{n_{\mathrm{gold}}^2}\frac{I_0(\chi_2' b)}{I_1(\chi_2' b)} = -\frac{\chi_3}{n_{\mathrm{surr}}^2}\frac{K_0(\chi_3 b)}{K_1(\chi_3 b)}. \qquad \text{[S2]}$$

Here, the transversal wavevectors are ${\chi_2'}^2 = \beta_{\mathrm{Co-SP}}^2 - n_{\mathrm{gold}}^2 k_0^2$ and $\chi_3^2 = \beta_{\mathrm{Co-SP}}^2 - n_{\mathrm{surr}}^2 k_0^2$, $\beta_{\mathrm{Co-SP}}$ is the propagation constant of the Co-SP mode, and $I_m(x)$ is the m^{th} order Modified Bessel function of the 1st kind.

As shown in Figure S1b, the WG mode gradually slows down due to the ever changing radius of the tip toward the apex (red dashed line). When the WG mode reaches a certain phase velocity that matches the Co-SP mode's phase velocity, it resonantly excites the Co-SP mode on the tip's outer gold surface.[5] At this point, some power of the WG mode is transferred to the Co-SP mode that is about 7% for the gold coating of 100 nm and $n_{surr} = 1$ (blue solid line in Figure S1b). Consequently, the resonantly excited Co-SP mode propagates toward the apex and gets localized providing a strong localized spot. The hotspot can be used for detecting and exciting samples during SNOM applications.

S2. COUPLING EFFICIENCY of PLANAR KRETSCHMANN CONFIGURATION

For the planar SPPs (P-SPPs) excited in planar Kretschmann configurations, [6,7] we calculate the coupling efficiency ($A_{\mathrm{P-SPP}}$) as follows

$$A_{\mathrm{P-SPP}} = 1 - r_{\mathrm{min}}. \quad \text{[S3]}$$

Here, the minimum reflectance, r_{min}, is obtained with Fresnel equation and calculated at the resonant incidence angle for each refractive index of a surrounding medium, n_{surr}.

S3. COUPLING ENHANCEMENT DEPENDING ON THE COATING THICKNESS

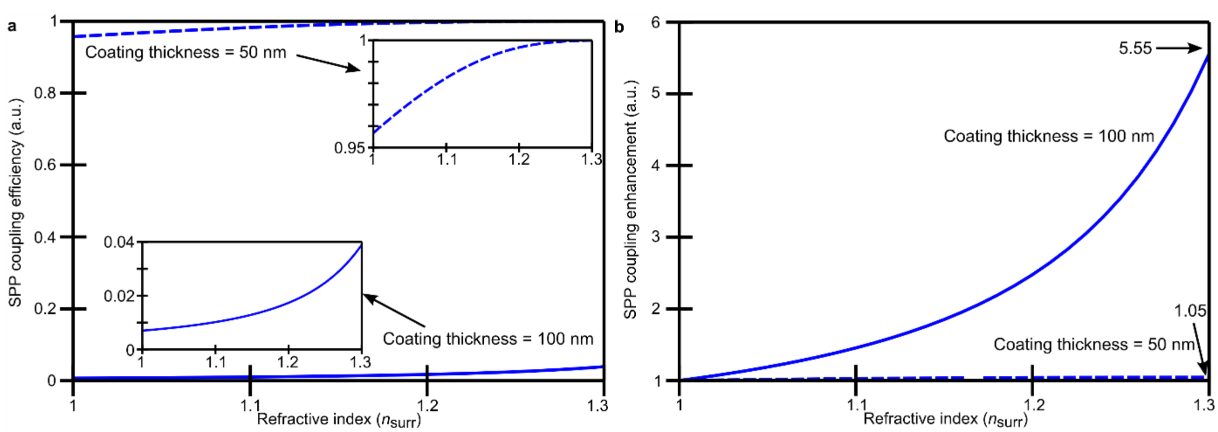

Figure S2. (a) SPP coupling efficiency depending on the surrounding medium's refractive index plotted for a coating thickness of 100 nm (solid line) and 50 nm (dashed line). Insets provide detailed information on the vertical scale of the individual curves. (b) SPP coupling enhancement factor vs. surrounding medium's refractive index plotted for a coating thickness of 100 nm (solid line) and 50 nm (dashed line).

S4. IMAGINARY PART of the EFFECTIVE INDEX

As the surrounding media gets optically dense, the Co-SP mode gets lossier and slower in the plasmonic tip. Figure S2a presents the imaginary part of the dispersion curves of TM_{01} waveguide (black curve) and TM_0 Co-SP modes. For the Co-SP mode, the surrounding medium are presented for air with $n_{surr} = 1$ (magenta curve), liquid with $n_{surr} = 1.3$ (green curve), and liquid with $n_{surr} = 1.71$ (orange curve). As the figure shows, the loss increases as the refractive index of the surrounding medium increases. Meanwhile, Figure S2b shows the normalized phase velocity (υ_{ph}/c, where c is the light velocity in vacuum) of TM_{01} waveguide (black curve) and TM_0 Co-SP modes in the above mentioned medium. The Co-SP mode slows down as it approaches toward the apex of the tip, and the velocity is smaller when the surrounding media refractive index is higher.

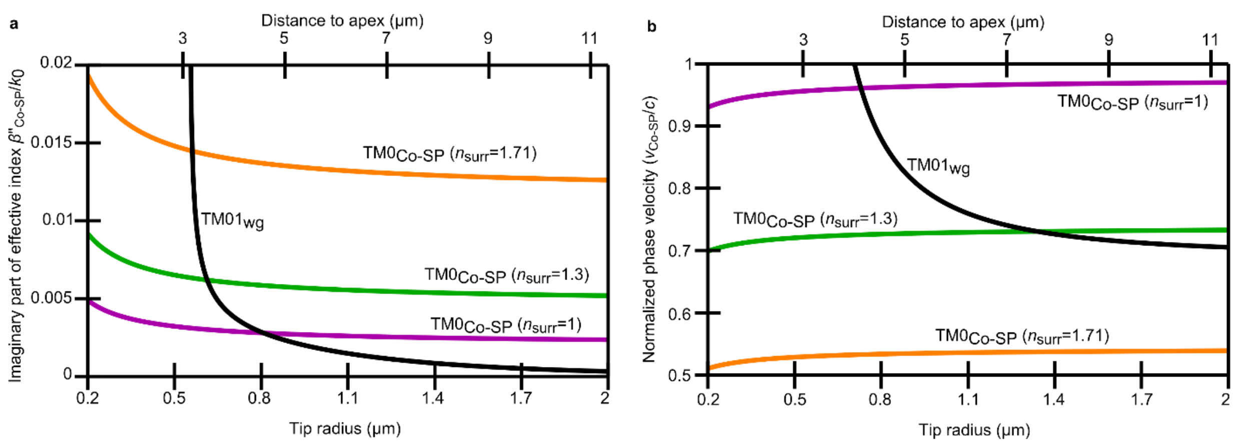

Figure S3. (a) Effective index's imaginary part for TM_{01} waveguide (black curve) and TM_0 Co-SP modes. For the Co-SP mode, the surrounding medium are presented for air with $n_{surr} = 1$ (magenta curve), liquid with $n_{surr} = 1.3$ (green curve), and liquid with $n_{surr} = 1.71$ (orange curve). TM_0 denotes the radially polarized Co-SP mode. (b) Normalized phase velocity (υ_{ph}/c) of TM_{01} waveguide (black curve) and TM_0 Co-SP modes for the above mentioned medium.

S5. SEM IMAGE of a CROSS SECTIONED TIP

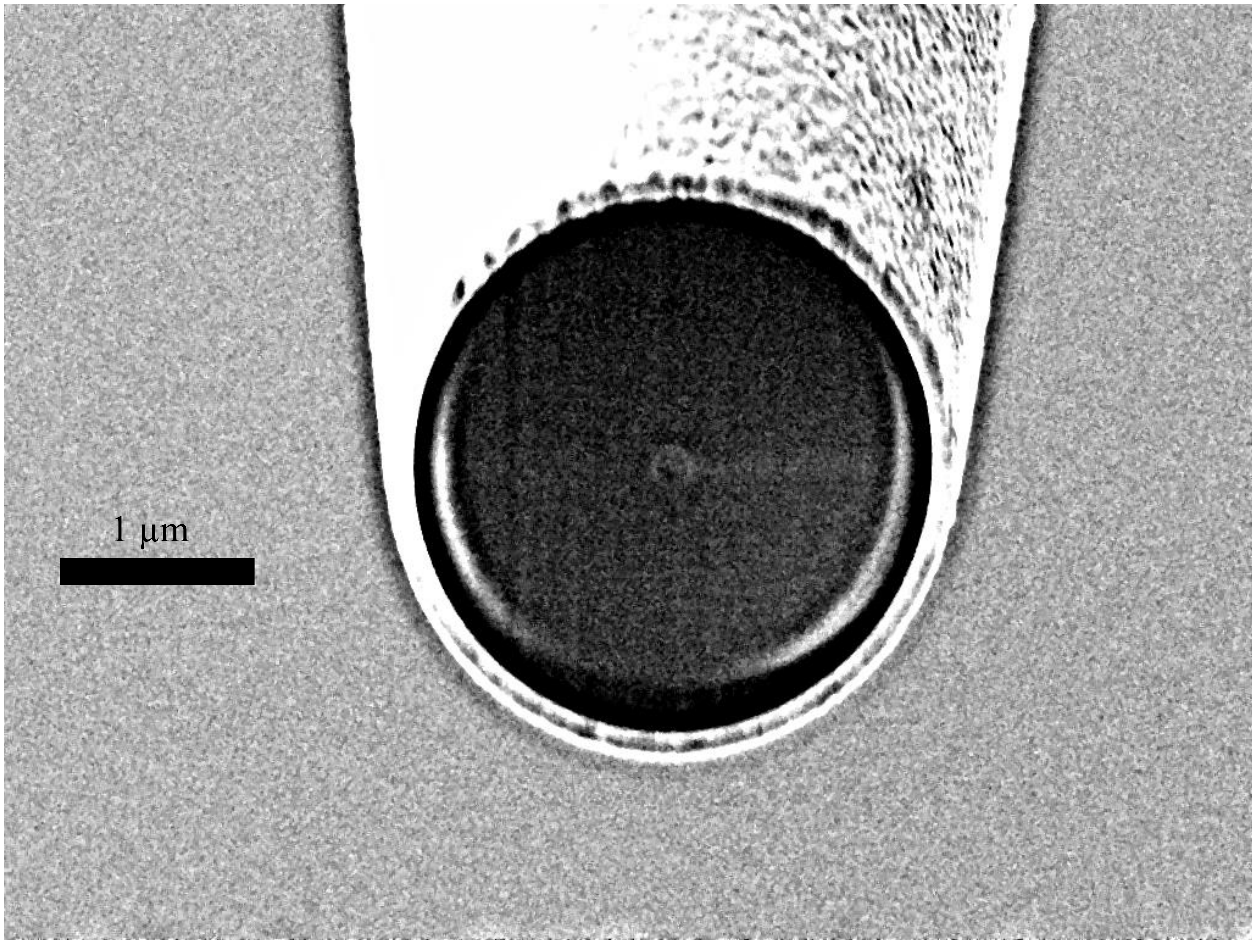

Figure S4. Scanning electron microscopy (SEM) image of the cross-sectioned tip with an aperture diameter of 3 μm. In the middle of the aperture, one can see the well preserved ring core of the vortex fiber that has shrunk from 9 μm to 200 nm.

REFERENCE

(1) Tugchin, B. N.; Janunts, N.; Klein, A. E.; Steinert, M.; Fasold, S.; Diziain, S.; Sison, M.; Kley, E.-B.; Tünnermann, A.; Pertsch, T. Plasmonic Tip Based on Excitation of Radially Polarized Conical Surface Plasmon Polariton for Detecting Longitudinal and Transversal Fields. *ACS Photonics* **2015**, *2*, 1468–1475.

(2) Novotny, L.; Hafner, C. Light Propagation in a Cylindrical Waveguide with a Complex, Metallic, Dielectric Function. *Phys. Rev. E* **1994**, *50*, 4094–4106.

(3) Rakic, A. D.; Djurišic, A. B.; Elazar, J. M.; Majewski, M. L. Optical Properties of Metallic Films for Vertical-Cavity Optoelectronic Devices. *Appl. Opt.* **1998**, *37*, 5271.

(4) Marcuse, D. *Light Transmission Optics*, 2nd ed.; Van Nostrand Reinhold Company Inc., 1982.

(5) Janunts, N.; Baghdasaryan, K.; Nerkararyan, K.; Hecht, B. Excitation and Superfocusing of Surface Plasmon Polaritons on a Silver-Coated Optical Fiber Tip. *Opt. Commun.* **2005**, *253*, 118–124.

(6) Kretschmann, E. Die Bestimmung optischer Konstanten von Metallen durch Anregung von Oberflächenplasmaschwingungen. *Zeitschrift für Phys.* **1971**, *241*, 313–324.

(7) Li, G.; Seshadri, S. R. Evanescent Wave Excitation of the Surface Polariton. *J. Appl. Phys.* **1990**, *67*, 22.